Ann. Anim. Sci., Vol. 23, No. 2 (2023) 461–471 *DOI: 10.2478/aoas-2022-0088*

sciendo

ANTIMICROBIAL IMPACTS OF ZINC OXIDE NANOPARTICLES ON SHIGA TOXIN-PRODUCING *ESCHERICHIA COLI* (SEROTYPE O26)

Rasha M. Sherif[1], Dalia Talat[2], Bothaina A. Alaidaroos[3], Reem M. Farsi[3], Shahira A. Hassoubah[3], Fatima A. Jaber[4], Treza M. Azer[1], Reham M. El-Masry[5], Mohamed E. Abd El-Hack[6], Madiha S. Ibrahim[2]•, Ahmed Elbestawy[7]

[1]Laboratory of Directorate of Veterinary Medicine, Kafr El-Sheikh, Egypt
[2]Department of Microbiology, Faculty of Veterinary Medicine, Damanhour University, Egypt
[3]Department of Biological Science, Faculty of Sciences, King Abdulaziz University, Saudi Arabia
[4]University of Jeddah, College of Science, Department of Biology, Jeddah 21589, Saudi Arabia
[5]Directorate of Veterinary Medicine, El-Gharbia, Egypt
[6]Poultry Department, Faculty of Agriculture, Zagazig University, Zagazig 44511, Egypt
[7]Department of Poultry and Fish Diseases, Faculty of Veterinary Medicine, Damanhour University, Egypt
•Corresponding author: madihasalah@vetmed.dmu.edu.eg

Abstract

The antibacterial activity of zinc oxide nanoparticles (ZnO NPs) has received significant attention worldwide due to the emergence of multidrug-resistant microorganisms. Shiga toxin-producing *Escherichia coli* is a major foodborne pathogen that causes gastroenteritis that may be complicated by hemorrhagic colitis or hemolytic uremic syndrome. Therefore, this study aimed to evaluate the antimicrobial effect of ZnO NPs against *E. coli* O26 and its Shiga toxin type 2 (*Stx2*). Multidrug resistance phenotype was observed in *E. coli* O26, with co-resistance to several unrelated families of antimicrobial agents. Different concentrations of ZnO NPs nanoparticles (20 nm) were tested against different cell densities of *E. coli* O26 (10^8, 10^6 and 10^5 CFU/ml). The minimum inhibitory concentration (MIC) value was 1 mg/ml. Minimum bactericidal concentration (MBC) was 1.5 mg/ml, 2.5 mg/ml and 3 mg/ml, respectively, depending on ZnO NPs concentrations and bacterial cell density. Results showed a significant (P≤0.05) decrease in *Stx2* level in a response to ZnO NPs treatment. As detected by quantitative real-time PCR, ZnO NPs down-regulated the expression of the *Stx2* gene (P≤0.05). Moreover, various concentrations of ZnO NPs considerably reduced the total protein content in *E. coli* O26. There was a significant reduction in protein expression with increased ZnO NPs concentration compared to the non-treated control. Scanning electron micrographs (SEM) of the treated bacteria showed severe disruptive effects on *E. coli* O26 with increasing ZnO NPs concentration. The results revealed a strong correlation between the antibacterial effect and ZnO NPs concentrations. ZnO NPs exert their antibacterial activities through various mechanisms and could be used as a potent antibacterial agent against *E. coli* O26.

Key words: ZnO NPs, *E. coli* O26, *Stx2*, protein expression, SEM

Nanotechnology focuses on creating and using materials with nanoscale spatial dimensions (Abd El-Hack et al., 2017 a, b, 2021 a; Islam et al., 2022). There have been conflicting views on nanomaterials, with some believing they are safe (Sungkaworn et al., 2007; Abd El-Hack et al., 2021 b) while others believe they are too harmful (Woodhouse, 2004). Zinc oxide (ZnO) is safe for humans and animals as reported by the US Food and Drug Administration (21CFR182.8991). It is being used in various biological applications such as drug delivery, bio-imaging probes, and cancer treatment (Akhtar et al., 2012; Al-Gabri et al., 2021). Zinc oxide nanoparticles (ZnO NPs) have antimicrobial activity (Sheiha et al., 2020; Alagawany et al., 2021; Yehia et al., 2022) against Gram-positive bacteria (Guo et al., 2015), Gram-negative bacteria (Reddy et al., 2014), spores germination and infectivity (Wagner et al., 2016) and fungi (Ramadan et al., 2016).

Several mechanisms of antibacterial action have been reported, including direct contact with cell walls which destroys bacterial cell integrity, resulting in the release of Zn ions and reactive oxygen species (ROS), leading to an oxidative effect (Makhluf et al., 2005; Zhang et al., 2010), damage of membrane cell wall through adhesion on the cell membrane (Stoimenov et al., 2002), penetration through the membrane cell wall (Makhluf et al., 2005) and cellular internalization of nanoparticles (Brayner et al., 2006). Multidrug-resistant *E. coli* is a major public health concern worldwide which causes serious infections (Hemeg, 2018). Shiga-toxigenic *E. coli* (STEC) impacts both animal and human health. The low infectious doses of STEC, in particular, were a major source of concern for public health (Murinda et al., 2019).

The STEC causes gastrointestinal illnesses (Bascheraa et al., 2019), acute renal failure, and foodborne outbreaks (Mohammadi et al., 2013). More than 70% of human non-O157 STEC infections are caused by STEC serogroup O26 (Shridhar et al., 2019). The virulence fac-

tors of *E. coli* O26, highly pathogenic strains carrying the Shiga toxin type 2 (*Stx2*) genes, have increased the incidence of hemolytic uremic syndrome (HUS) (Delannoy et al., 2015). The genes coding for *Stx2* are the primary virulence factor of all STEC that causes a wide range of diseases, including hemorrhagic colitis and HUS (Lee et al., 2016), affecting neuronal function and leading to paralysis (Obata et al., 2008), gastroenteritis, urinary tract infections, neonatal meningitis, Crohn's disease (Lim et al., 2017), severe systemic complications and death (Stromberg et al., 2015).

ZnO NPs can potentially prevent STEC infection and the expression of adhesins, virulence factors, and *Stxs* (Crane et al., 2014). Yusof et al. (2019) recommended ZnO NPs as a perfect, safe and outstanding antimicrobial drug alternative. ZnO NPs differ from bulk ZnO. ZnO NPs are better in many commercial processes due to their small size and high surface area. Also, using ZnO NPs reduces the total amount of applied ZnO, enabling the development of special applications in all fields of expertise (Nemček et al., 2020).

The current work aimed to assess the antimicrobial activity of ZnO NPs against *E. coli* O26 and the *Stx2* in qualitative and quantitative methods. This work investigated the effects on the cellular level by SEM of *E. coli* O26 treated with ZnO NPs.

Material and methods

Bacterial strain

E. coli O26 was biochemically and serologically identified by Animal Health Research Institute. The specific primers combinations were used to detect the *Stx2* gene in *E. coli* O26 as shown in Table 1 (Dipineto et al., 2006).

Preparation of zinc oxide nanoparticles suspension

ZnO NPs with a size of 20 nm were purchased from Sigma-Aldrich Corporation (St. Louis, MO, USA) and different concentrations (0.1, 0.2, 0.3, 0.4, 0.5, 1, 1.5, 2, 2.5, 3, 3.5 and 4 mg/ml) were prepared. ZnO powder and nanoparticles (0.1 g) were initially sterilized at 160°C for 3 h, then dispersed in 25 ml ultrapure water (Milli-Q®, Millipore Corporation, Bedford, MA, USA), vigorously vortexed for 10 min, then sonicated for 30 min to avoid aggregation and deposition of particles. The resulting suspension (4 mg/ml) was used as a stock solution for bacterial susceptibility evaluation (Tayel et al., 2011).

Antimicrobial susceptibility testing

E. coli O26 was tested for its susceptibility against a panel of 16 antibiotics using the disk diffusion method according to the guidelines of the Clinical Laboratory Standard Institute (CLSI, 2020). The following antimicrobials were tested: ampicillin + sulbuctam (20 µg), colistin (10 µg), cephradine (30 µg), ciprofloxacin (5 µg), enrofloxacin (5 µg), nitrofurantoin (300 µg), doxycycline (30 µg), sulpha-trimethoprime (25 µg), spiramycin (100 µg), spectinomycin (100 µg), nalidixic acid (30 µg), neomycin (10 µg), gentamycin (10 µg), amoxycillin (25 µg), azithromycin (15 µg) and clindamycin (2 µg). Inhibition zone diameters were measured in mm.

Determination of Minimum Inhibitory Concentration (MIC)

MIC of ZnO NPs was performed according to ESCMID (2000). Overnight, broth cultures of *E. coli* O26 were briefly suspended in sterilized Tryptic Soy Broth (TSB) (Sigma-Aldrich Corporation, St. Louis, MO, USA). Two hundred µl of bacterial culture (10^8, 10^6 and 10^5 CFU/ml) were mixed with ZnO NPs at different concentrations (0.1, 0.2, 0.3, 0.4, 0.5, 1, 1.5, 2, 2.5, 3, 3.5 and 4 mg/ml). The tubes were incubated for 24 h at 37°C. TSB medium with the tested bacterial concentrations and negative control was used. The MIC was determined by observing the visual turbidity of the tubes before and after incubation. We repeated the experiments three successive times.

Determination of Minimum Bactericidal Concentration (MBC)

Plates were incubated at 37°C for 24 h. From each tube containing 24 h incubated bacterial culture with different ZnO NPs concentrations, 50 µl was streaked on the surface of sterilized MacConkey agar (Sigma-Aldrich Corporation, St. Louis, MO, USA). The MBC was the least concentration of ZnO NPs that prevented the growth of bacteria on antibiotic-free culture media according to Alekish et al. (2018).

Determination of total protein using sodium dodecyl sulphate polyacrylamide gel electrophoresis (SDS-PAGE)

Different cell densities of *E. coli* O26 (10^8, 10^6 and 10^5 CFU/ml) were treated with various ZnO NPs (MIC value, MBC value and 3.5 mg/ml). The effect of ZnO NPs on protein synthesis was performed according to Ghazi et al. (2009). The stored lysed samples were brought to complete protein extraction. Cell debris was removed by centrifugation at ~16,000^{x}g for 30 minutes at 4°C. The supernatant was transferred to a new tube for further protein concentration determination analysis. A Bradford assay was performed according to the manufacturer's instructions. Twenty (ug) protein concentration of each sample was loaded with an equal volume of 2x Laemmli sample buffer. The sample was separated on a polyacrylamide gel. Each of the previous mixtures was boiled at 95°C for 5 min and then subjected to polyacrylamide gel electrophoresis. TGX Stain-Free™ FastCast™ Acrylamide Kit (SDS-PAGE) provided by Bio-Rad Laboratories, TNC, USA Catalog. NO. 161-0181 was used and prepared according to the manufacturer's instructions.

Scanning electron microscope (SEM) analysis

SEM was used to examine the morphological changes of *E. coli* O26 before and after ZnO NPs treatment ac-

cording to Tayel et al. (2011). Cells were primarily fixed with fixative buffer (2.5% glutaraldehyde, 2% paraformaldehyde in 0.1 M Na-cacodylate buffer, pH 7.35) for 30 min. Then, they were rinsed three times with ultrapure water before being dehydrated using a series of ethanol solutions, dried, mounted on SEM tubs, and sputter-coated with gold/palladium, then examined.

Detection of Shiga toxin type 2 (Stx2) production using Enzyme-Linked Immunosorbent Assay (ELISA)

To investigate the effect of ZnO NPs on *Stx2* production, an indirect ELISA based on the recognition of *Stx2* by specific antibodies was performed as described by USDA-FSIS Guidebook. Different cell densities of *E. coli* O26 (10^8, 10^6, and 10^5 CFU/ml) were treated with various ZnO NPs (MIC value, MBC value and 3.5 mg/ml). *E. coli* O26 consisting of stationary-phase cells were obtained by inoculating tryptic soy broth with a single colony from a tryptic soy agar plate and adding different ZnONPs concentrations, followed by incubation with shaking at 37°C for 10 h. Hundred µL of the control solutions and samples were loaded into the wells of the test strips. Analysis in triplicate was done according to the manufacturer's instructions. An anti-*Stx2* antibody was used. Absorbance was read at 450 nm using a microplate ELISA photometer.

Measuring Stx2 gene expression using quantitative real-time PCR (qPCR) analysis

To investigate the effect of ZnO NPs on the expression of the *Sxt2* gene, qPCR was performed according to Chen et al. (2013). According to the manufacturer's instruction, total RNA was extracted using RNA extraction kit (Thermo Scientific, Fermentas, #K0731). The housekeeping gene (RpoB) is represented as normalization and is used to calculate the relative gene expression or fold change in the target gene. Therefore, the quantities critical threshold (Ct) of the target gene was normalized with quantities (Ct) of the housekeeping gene (RpoB) by using the 2-ΔΔCt method (Livak and Schmittgen, 2001). The qPCR with SYBR Green was used to measure the expression of the *Stx2* gene, with *RpoB* as an internal reference. The primers used are shown in Table 2.

Statistical analysis

All the data were expressed as means ±SE. The statistical significance was evaluated by one-way analysis of variance (ANOVA) using SPSS, 18.0 software (2011) and the individual comparisons were obtained by Duncan's multiple range tests. Values were considered statistically significant when $P \leq 0.05$, according to Ross and Willson (2017).

Results

Molecular detection of Shiga toxin type 2 (Stx2) gene

Specific primers were used to detect the expression of the *Stx2* gene in *E. coli* O26. Positive amplification of 779 bp fragments specific to the *Stx2* gene in *E. coli* O26 is shown in Figure 1.

Antimicrobial susceptibility testing

As illustrated in Table 3, *E. coli* O26 showed high resistance to 10 (62.5%) of the tested antimicrobials: doxycycline, sulpha-trimethoprim, spiramycin, spectinomycin, nalidixic acid, neomycin, gentamycin, amoxicillin, azithromycin and clindamycin. However, the highest sensitivity was observed with the penicillin+β-lactamase inhibitor group of antibiotics and polymyxin E group, followed by ciprofloxacin, enrofloxacin, nitrofurantoin and cephradine.

Determination of Minimum Inhibitory Concentration (MIC) and Minimum Bactericidal Concentration (MBC) of ZnO NPs against *E. coli* O26

The antibacterial activity of ZnO NPs against *E. coli* O26 was investigated using MIC and MBC assays. The growth of *E. coli* O26 (10^8, 10^6 and 10^5 CFU/ml) was individually assessed with different concentrations of ZnO NPs (0.1, 0.2, 0.3, 0.4, 0.5, 1, 1.5, 2, 2.5, 3, 3.5 and 4 mg/ml) after 24 h. MIC value of ZnO NPs against *E. coli* O26 was 1 mg/ml with different cell densities. The MBC of ZnO NPs was 1.5 mg/ml, 2.5 mg/ml and 3 mg/ml, depending on bacterial cell density and ZnO NPs concentration, as shown in Table 4. The antibacterial activity of ZnO NPs increased as the concentration of zinc oxide nanoparticles increased.

Table 1. Oligonucleotide primers sequences used for the detection of *Stx2* gene in *E. coli* O26

Gene	Primer sequence (5'-3')	Length of amplified product	Reference
Stx2	CCATGACAACGGACAGCAGTT CCTGTCAACTGAGCAGCACTTTG	779 bp	Dipineto et al. (2006)

Table 2. Forward and reverse primers sequences for *Stx2* and *RpoB* genes used in qPCR assay

Target gene	Forward primer	Reverse primer	Size (bp)	Reference
Stx2	/5 CTTCGGTATCCTATTCCC/3	/5 GGGTGTGGTTAATAACAG/3	150	Chen et al. (2013)
RpoB	/5 CAACCTGTTCGTACGTATC/3	/5 CTCTGTGGTGTAGTTCAG/3	79	

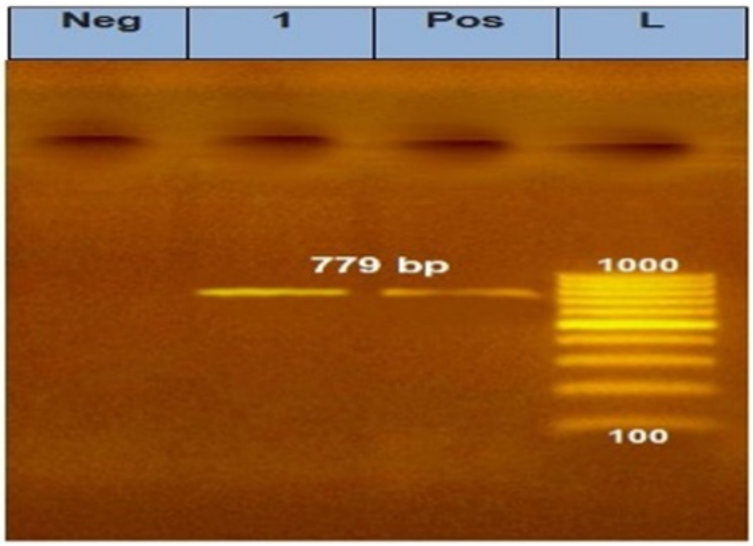

Figure 1. Detection of *stx2* gene by specific primers. L: Molecular weight marker, POS: Positive control, 1: PCR product of *Stx2* gene tested *E. coli* O26 and Neg: negative control

Table 3. Antimicrobial susceptibility testing of *E. coli* O26 showing high multidrug resistance

Antimicrobial agent	Concentration (μg)	Inhibition zone diameter (cm)	Interpretation
Ampicillin + sulbuctam (SAM)	20	1.4	
Colistin (CL)	10	1.2	S
Cephradine (CE)	30	1.5	I
Ciprofloxacin (CIF)	5	1.7	I
Enrofloxacine (EX)	5	1.7	I
Nitrofrontoin (F)	300	1.6	I
Neomycin (N)	10	0.9	R
Gentamycin (CN)	10	0.8	R
Nalidixic Acid (NA)	30	0	R
Clindamysin (DA)	2	0	R
Azithromycin (AZM)	15	1.3	R
Spectinomycin (SPT)	100	1.5	R
Spiramycin (SR)	100	0	R
Amoxycillin (AX)	25	0	R
Sulphatrimethoprime (SXT)	25	0	R
Doxycycline (DO)	30	0.9	R

S: Sensitive; I: Intermediate; R: Resistance.

Table 4. The MIC and MBC of ZnO NPs against *E. coli* O26

E. coli O26 (CFU/ml)	MIC (mg/ml)	MBC (mg/ml)
10^8	1	1.5
10^6	1	2.5
10^5	1	3

Effect of different ZnO NPs concentrations on protein expression in *E. coli* O26

The total protein concentration in *E. coli* O26 (10^8, 10^6 and 10^5 CFU/ml) treated with various concentrations of ZnO NPs (MIC concentration, MBC concentration and 3.5 mg/ml) and untreated control showed that the concentration of total protein decreased as the concentration of ZnO NPs increased, as illustrated in Figures 2 A, B and C.

SDS-PAGE analysis of the control and ZnO NPs treated *E. coli* O26 was performed. We found that the electrophoretic patterns were altered as the concentration

of ZnO NPs varied compared to the untreated control, revealing clear polypeptide bands. At 1 mg/ml ZnO NPs concentration, the number and intensity of protein bands decreased and faded, whereas at MBC concentration and 3.5 mg/ml ZnO NPs concentrations, no bands appeared, as shown in Figures 3 A, B and C.

Scanning electron microscope (SEM)

The interaction between ZnO NPs and *E. coli* O26 was evaluated by SEM image analysis as shown in Figure 4. SEM analysis of *E. coli* O26 without ZnO NPs treatment (control) showed a rod with a length of 1–3 µm and an average diameter of 0.5–1 µm (Figure 4 A). The arrangement was mostly single or in groups. At 0.5 and 1 mg/ml of ZnO NPs, damage to the membrane envelope components, different shapes in treated cells and the formation of irregular cell surfaces were noticed. Also, few remaining intact cells were seen in a pond of released internal cell components (Figure 4 B). At 2.5 and 3 mg/ml of ZnO NPs, different shapes were found in the treated cells showing the ascendency of coccoid forms and the formation of irregular cell surfaces. At 3.5 mg/ml and 4 mg/ml of ZnO NPs, there was a difference in length, diameter and arrangements of treated cells by approximately 0.1–0.2 µm due to many softened, broadened, lysed cells with their internal components released, leading to the death of the cells, as shown in Figure 4 D.

Effect of different concentrations of ZnO NPs on Stx2 production by *E. coli* O26

ELISA was performed to assess the effect of ZnO NPs on *Stx2* production. As shown in Figures 5 A, B and C, a significant ($P \leq 0.05$) decrease in *Stx2* level was found in the treated *E. coli* O26 (10^8, 10^6 and 10^5 CFU/ml) with varying concentrations of ZnO NPs (MIC concentration, MBC concentration and 3.5 mg/ml) compared to the untreated control. When the concentration of ZnO NPs was 3.5 mg/ml, the lowest production of *Stx2* was detected with the different cell densities of *E. coli* O26. No significant differences were noticed between G3 (ZnO NPs concentration was the MBC value) and G4 (ZnO NPs concentration was higher than MBC concentration, 3.5 mg/ml).

Effect of different concentrations of ZnO NPs on Stx2 gene expression by qPCR

The expression level of the *Stx2* gene in all tested *E. coli* O26 densities (10^8, 10^6 and 10^5 CFU/ml) following exposure to different ZnO NPs levels (0–3.5 mg/ml) was determined by qPCR. Figures 6 A, B, and C showed significant down-regulation of the *Stx2* gene following exposure to different concentrations of ZnO NPs compared to the untreated control. The lowest expression of the *Stx2* gene was noticed when the concentration of ZnO NPs was 3.5 mg/ml with various cell densities of *E. coli* O26.

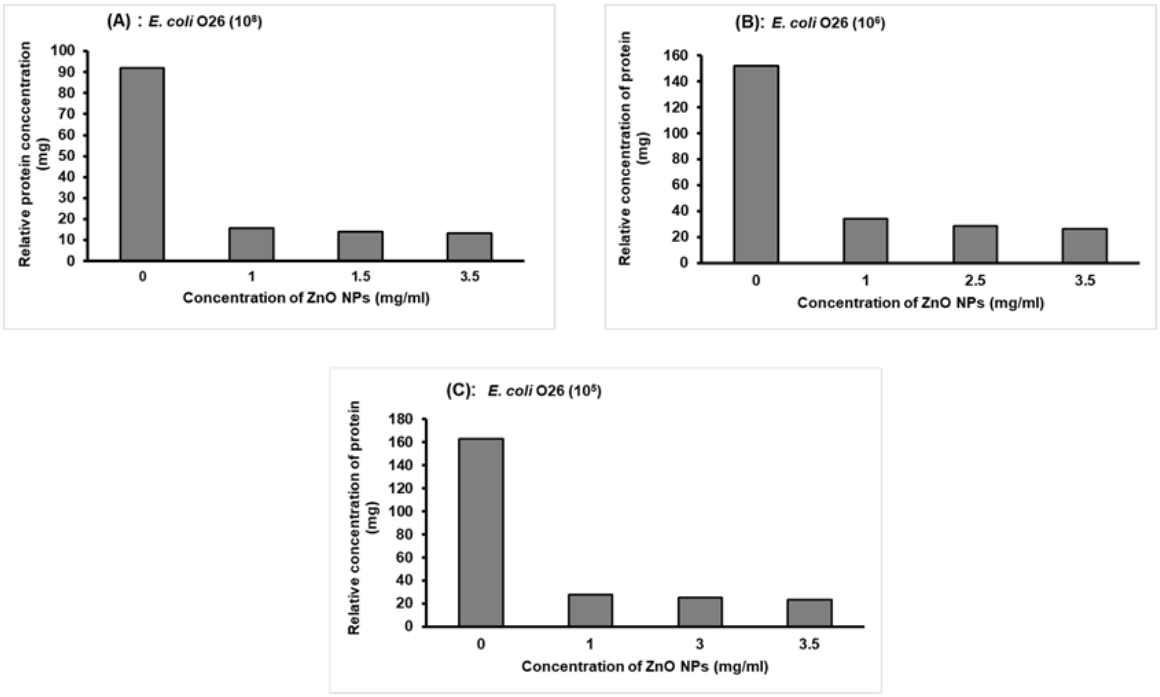

Figure 2. Effect of various concentrations of ZnO NPs on the total protein content of *E. coli* O26 (A: 10^8, B: 10^6 and C: 10^5 CFU/ml) following treatment with different concentrations of ZnO NPs (0–3.5 mg/ml), *P<0.05

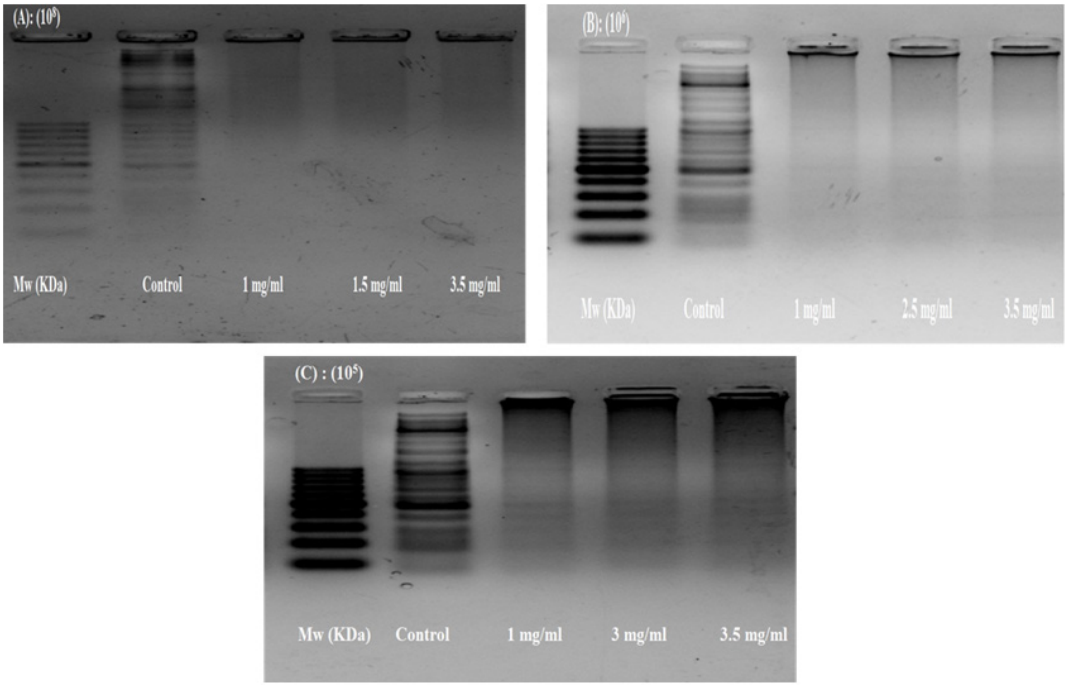

Figure 3. SDS-PAGE analysis of the protein expression in *E. coli* O26 (A: 10^8, B: 10^6, and C: 10^5 CFU/ml before (control) and after incubation with various concentrations of ZnO NPs (0–3.5 mg/ml). 2, control: *E. coli* O26 without treatment with ZnO NPs; 3, *E. coli* O26 treated with ZnO NPs at 1 mg/ml; 4, *E. coli* O26 treated with ZnO NPs at 1.5 mg/ml for (10^8 CFU/ml), 2.5 mg/ml for (10^6 CFU/ml) and 3 mg/ml for (10^5 CFU/ml); 5, *E. coli* O26 treated with ZnO NPs at 3.5 mg/ml

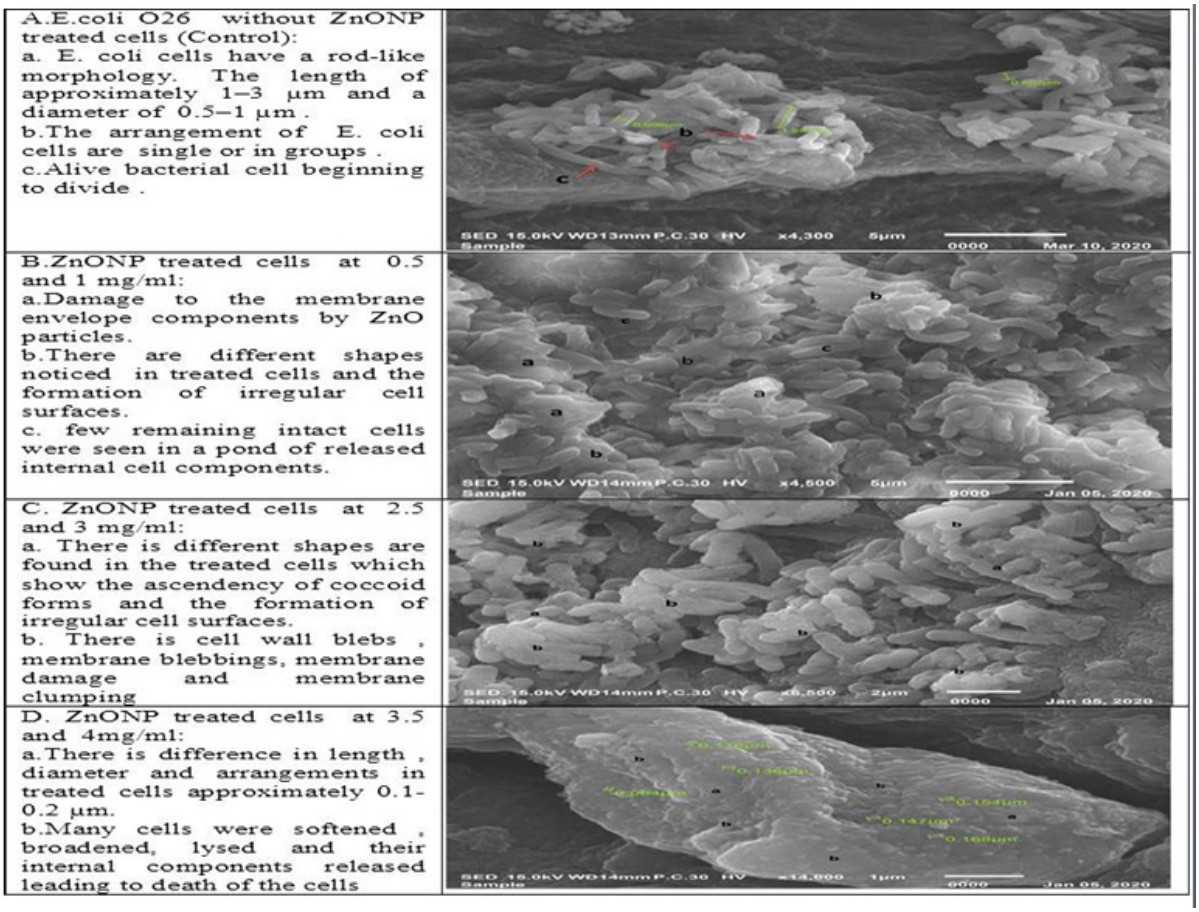

Figure 4. Scanning electron microscopy (SEM) images show morphological alterations in *E. coli* O26 following treatment with different concentrations of ZnO NPs. (A): non-treated; (B): 0.5–1 mg/ml ZnO NPs; (C): 2.5–3 mg/ml ZnO NPs; (D): 3.5–4 mg/ml ZnO NPs

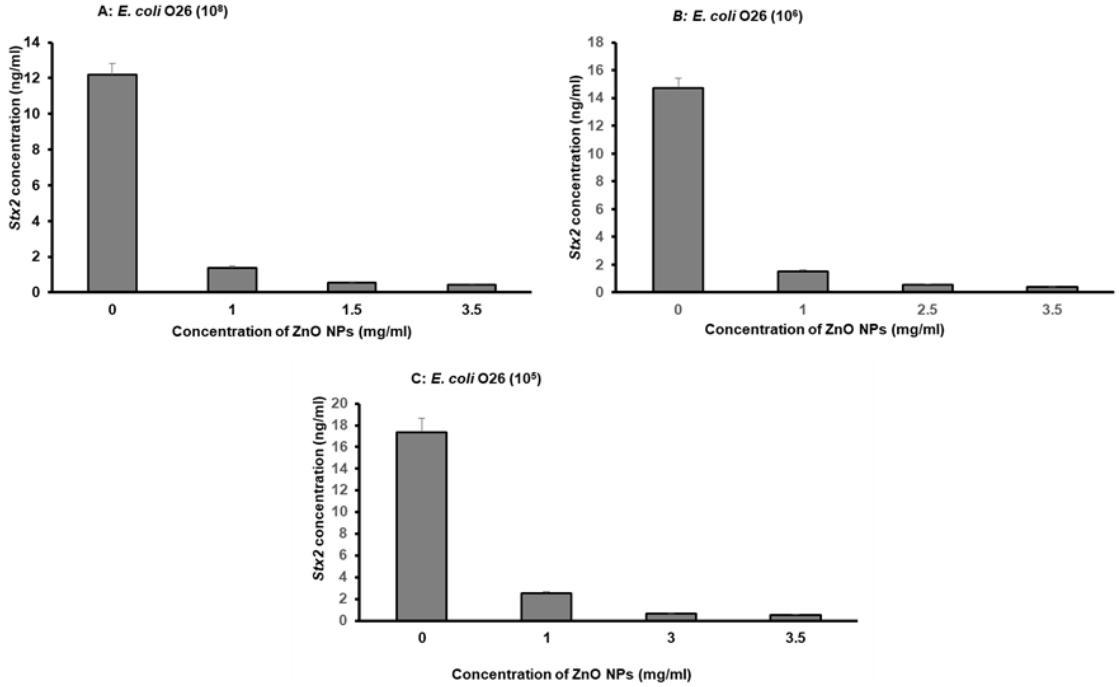

Figure 5. Quantitative measurement of *Stx2* production of *E. coli* O26 A: (10^8 CFU/ml), B: (10^6 CFU/ml) and C: (10^5 CFU/ml) CFU/ml following treatment by different concentrations of ZnO NPs (0–3.5 mg/ml) by an ELISA, *P<0.05

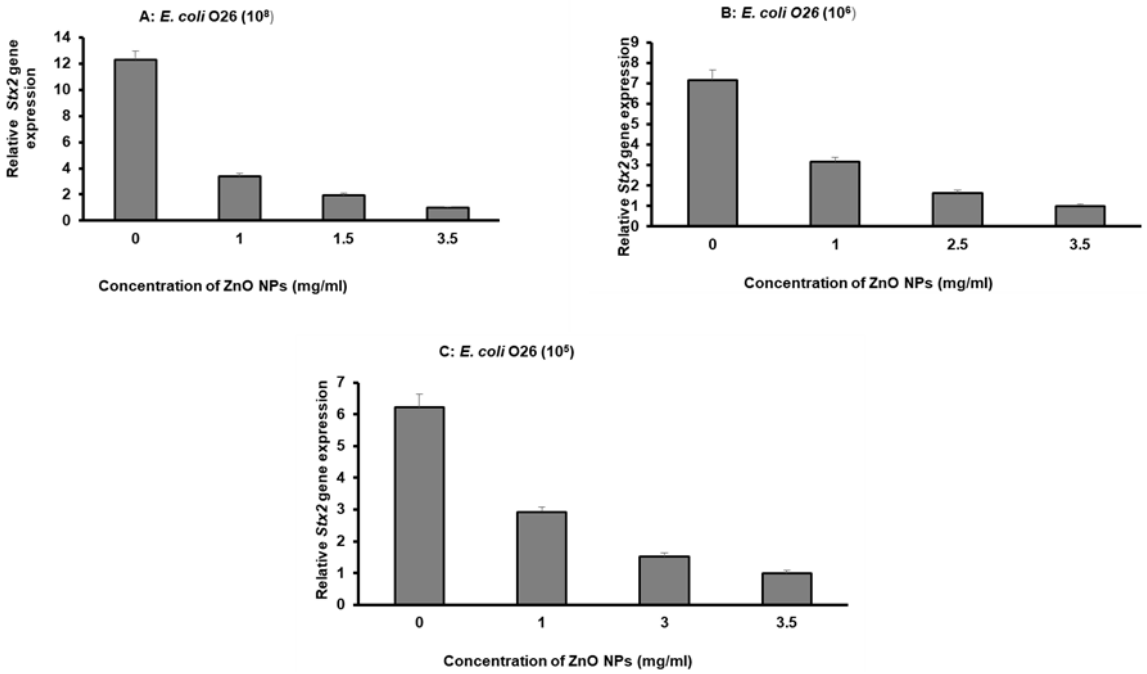

Figure 6. qPCR analysis of the expression of *Stx2* gene in *E. coli* O26 A: (10^8 CFU/ml), B: (10^6 CFU/ml) and C: (10^5 CFU/ml) following treatment with different concentrations of ZnO NPs (0–3.5 mg/ml). The expression level of the target gene in non-treated control was considered the baseline, *P<0.05

Discussion

The emergence and widespread occurrence of multidrug-resistant pathogenic bacteria are becoming a global public health concern. *E. coli* is becoming increasingly resistant to multiple antibiotics, hindering the therapeutic management of infections (Hemeg, 2018). Recently, metal oxide nanomaterials have exhibited superior antibacterial activity against multidrug-resistant microorganisms (Ashour et al., 2020; El-Tarabily et al., 2021; Mwaheb et al., 2021). There are some concerns that the application of metal nanoparticles could accelerate the

development of metal-resistant bacteria leading to the development of antimicrobial resistance mechanisms as reported that strains of *E. coli* evolved Ag-NP resistance by overproducing flagellin, the main flagella protein to facilitate NP aggregation and immobilization outside cells but overcome by adding inhibitors of flagellin production (Amaro et al., 2021). Thus, this study investigated the antibacterial effect of ZnO NPs against the Shiga toxigenic strain (*E. coli* O26) and the mechanisms by which ZnO NPs can influence the viability of *E. coli* O26 and Stx2 toxicity. ZnO NPs showed a high therapeutic potential (Anjum et al., 2021; Abd El-Hack et al., 2017, 2021 a; Al-Gabri et al., 2021).

E. coli O26 was assessed for its susceptibility to 16 antimicrobial agents. Substantial resistance rates to various antimicrobial classes were detected in Table 3. *E. coli* O26 showed resistance to doxycycline, sulphatrimethoprim, spiramycin, spectinomycin, nalidixic acid, neomycin, gentamycin, amoxicillin, azithromycin and clindamycin. However, it is sensitive to ampicillin + sulbuctam and colistin. These results are consistent with numerous previous studies that reported multidrug-resistant STEC worldwide (Cergole-Novella et al., 2011; Meng et al., 2014; Hemeg, 2018; Rubab and Oh, 2020). However, few previous data reported low resistance in STEC as Day et al. (2016). They studied antimicrobial resistance in STEC serogroup O26 isolated from human cases of diarrheal disease in England between June 2015 and January 2016 and found that 82.6% and 64.7% of the isolates, respectively, lacked identifiable resistance genes and were predicted to be fully susceptible to 11 different classes of antimicrobials. Lajhar et al. (2017) determined the antimicrobial resistance phenotype of *E. coli* O26 isolated from cattle and clinical sources in Australia and a low level (13.6%) of antimicrobial resistance was observed.

The substantial antibiotic resistance identified in STEC creates a serious threat to the future control of STEC infections. It necessitates a need for a powerful alternative to these antibiotics. Different concentrations of ZnO NPs (20 nm) were used to determine the best concentration for the antibacterial activity against *E. coli* O26. As shown in Table 4, MIC of ZnO NPs on *E. coli* O26 with infective doses 10^8, 10^6 and 10^5 CFU/ml was 1 mg/ml in all doses and the MBC was 1.5, 2.5 and 3 mg/ml, respectively, under the same experimental conditions. This indicates that ZnO NPs have antimicrobial properties against *E. coli* O26. The antibacterial activity of ZnO NPs increased as the concentration of NPs increased. These results agree with previous studies that found that ZnO NPs have antibacterial activity against *E. coli* (Liu et al., 2009; Wang et al., 2012; Torabi, 2017; Alam, 2021). Liu et al. (2009) reported that 3 mmol/l ZnO NPs could inhibit the growth of *E. coli* O157:H7 and 12 mmol/l or higher concentrations completely inhibited the growth.

Furthermore, Wang et al. (2012) found that MIC and MBC for *E. coli* K88 were 0.1 and 0.8 µg/ml. Farzana et al. (2017) reported MIC value of 0.08 mg/ml for *E. coli*. Şahin et al. (2017) showed that 60 µg/ml ZnO NPs was sufficient against Gram-negative bacteria (*E. coli* ATCC25922, *E. coli* O157:H7). Also, Ahmed et al. (2019) reported the same results with MIC of 1.0 mg/ml and MBC of 1.5 mg/ ml. Hozyen et al. (2019) found that MIC and MBC values for *E. coli* were 5 mg/ml and 10 mg/ml, respectively. Differences in MIC and MBC values for *E. coli* may be due to the difference in the type of bacterial isolate and its concentration, in addition to the differences in size, concentration, crystal morphology of ZnO NPs and the methodology used for preparation.

The antibacterial activity of ZnO NPs increased as the concentration of NPs increased. Based on this result, ZnO nanoparticles have an antibacterial effect against *E. coli* O26. Narayanan et al. (2012) reported that even low concentrations of ZnO NPs had strong antibacterial activity on pathogenic *E. coli.* While some researchers argued that the antibacterial concentrations of ZnO NPs were safe to a certain level but toxic at higher concentrations to pathogenic *E. coli* (Bratz et al., 2013; Ibrahim et al., 2017). However, Sikora et al. (2018) and Matuła et al. (2019) found that bacteria could regrow and that the nano-rods were not as strong as the antibiotic treatment because the used strain showed several problems while studying.

Transcriptomic and proteomic analysis has been widely used in studying the molecular mechanisms of the action of antibacterial agents (Khodadadi et al., 2020; Tsakou et al., 2020). The role of nanoparticles in bacterial protein synthesis has received much interest in recent years. Nanoparticles can prevent bacteria from synthesizing protein and DNA by suppressing ATPase activities to lower ATP levels and preventing the ribosome subunit from binding tRNA (Cui et al., 2012; Alagawany et al., 2021; Yehia et al., 2022).

To investigate the effect of ZnO NPs on protein synthesis, the total protein content in *E. coli* O26 (10^8, 10^6, and 10^5 CFU/ml) treated with various concentrations of ZnO NPs and untreated control was assessed. As shown in Figure 2, the total protein concentration in *E. coli* O26 (10^8, 10^6, and 10^5 CFU/ml) declined as ZnO NPs level increased. Next, the total proteins of the control and ZnO NPs-treated with *E. coli* O26 were analyzed using SDS-PAGE. Compared to the untreated control, protein expression was greatly affected as the concentration of ZnO NPs changed. The number and intensity of protein bands dropped and faded at 1 mg/ml ZnO NPs. However, no bands were seen at 3.5 mg/ml ZnO NPs as shown in Figure 3. Although these proteins were not further characterized, qualitative gels revealed a substantial variation in the protein profile of control and ZnO NPs-treated cells. The lack of protein detection on exposure to higher concentrations might be due to the interference of ZnO NPs with the protein synthesis process, as previously reported (Babele, 2019; El-Sayed et al., 2019; Singh et al., 2019; Li et al., 2020).

A scanning electron microscope was performed to detect the morphology and cellular composition changes in *E. coli* O26 after treatment with ZnO NPs and their mechanism of action. In lower concentrations of ZnO NPs, abrasion and penetration of ZnO particles through the cell envelope were observed, leading to damage in the membrane envelope components. Few remaining intact cells were seen in a pond of released internal cell components. At higher concentrations, the ascendence of coccoid forms, formation of irregular cell surfaces and many cells softened, broadened, and lysed with their internal components released, leading to the death of the cells after less than 24 h of exposure. Thus, SEM images provided evidence of damage to bacterial cells after exposure to ZnO NPs which agree with Zhang et al. (2010), Tayel et al. (2011), Thangam et al. (2014), Manzoor et al. (2016), Dobrucka et al. (2018), Siddiqi et al. (2018), Awwad et al. (2020) and Naskar et al. (2020). Liu et al. (2009) reported no morphological changes; however, the reasons for that were unknown. Shiga toxin (*Stx*) is the major virulence factor of Shiga toxin-producing *E. coli* (STEC) and plays a significant role in *E. coli* pathogenesis. Zinc inhibits some pathogens' virulence factor expression and may be pathogen-specific (Patel et al., 2010; Sheiha et al., 2020).

To our knowledge, no study determined the effect of ZnO NPs on Shiga toxin production. Therefore, *Stx2* was measured by ELISA to detect whether ZnO NPs could affect *Stx2* production. Figure 5 shows a significant ($P \leq 0.05$) decrease in *Stx2* level in *E. coli* O26 treated with various concentrations of ZnO NPs. Thus, ZnO NPs suppressed Shiga toxin production. This result is supported by the finding of Uemura et al. (2017), who reported a significant reduction in the cytotoxic activity of *Stx2* in zinc-supplemented media compared to the control. Also, quantitative real-time PCR (qPCR) was performed to detect the *Stx2* gene. Figure 6 showed that ZnO NPs down-regulated the expression of the *Stx2* gene, and there was a strong correlation between the down-regulation of the *Stx2* gene and ZnO NPs concentrations. These results agree with previous studies that clarified that zinc exerts inhibitory effects on STEC strains and *Stx* expression (Crane et al., 2011, 2014; Uemura et al., 2017).

Conclusion

In conclusion, a multidrug resistance phenotype was observed in *E. coli* O26, with co-resistance to several unrelated families of antimicrobial agents. ZnO NPs treatment caused a significant decrease in *Stx2* level and down-regulated the expression of the *Stx2* gene. Moreover, various ZnO NPs levels considerably reduced the total protein content in *E. coli* O26. ZnO NPs showed severe disruptive effects on *E. coli* O26 with increasing ZnO NPs concentration. These results could lead us to consider ZnO NPs as the next-generation antibiotic alternative against multidrug-resistant pathogenic *E. coli*. However, further *in vivo* studies are still needed to confirm these antibacterial activities and to determine the safe doses of ZnO NPs to animal cells.

Ethical statement

The study was reviewed and approved by the Institutional Committee of Ethics and Research of Damanhour University, Egypt.

Data availability statement

All research data, methodology and results are available with all authors and can be easily requested through emails.

Author Contributions

RS, DT, RME and TA characterized the zinc oxide nanoparticles under the supervision of MI. RS, DT, and TA performed the antimicrobial susceptibility testing, determined MIC and MBC, applied SDS-PAGE, SEM analysis and ELISA under the supervision of MI and AE., RS, DT, BAA, RMF, FAJ, SAH, MEAE-H and TA wrote the manuscript. MI, FAJ and AE revised the manuscript, tables and figures. All authors contributed to the article and approved the submitted version.

Conflicts of Interest

The authors declare no conflict of interest.

References

Abd El-Hack M.E., Alagawany M., Farag M.R., Arif M., Emam M., Dhama K., Sayab M. (2017 a). Nutritional and pharmaceutical applications of nanotechnology: Trends and advances. Inter. J. Pharmacol., 13: 340–350.

Abd El-Hack M.E., Alagawany M., Arif M., Chaudhry M.T., Emam M., Patra A. (2017 b). Organic or inorganic zinc in poultry nutrition: a review. World's Poult. Sci. J., 73: 904–915.

Abd El-Hack M.E., El-Saadony M.T., Saad A.M., Salem H.M., Ashry N.M., Ghanima M.M.A., El-Tarabily K.A. (2021 a). Essential oils and their nanoemulsions as green alternatives to antibiotics in poultry nutrition: a comprehensive review. Poultry Sci., 101584.

Abd El-Hack M.E., Alaidaroos B.A., Farsi R.M., Abou-Kassem D.E., El-Saadony M.T., Saad A.M., Ashour E.A. (2021 b). Impacts of supplementing broiler diets with biological curcumin, zinc nanoparticles and *Bacillus licheniformis* on growth, carcass traits, blood indices, meat quality and cecal microbial load. Animals, 11: 1878.

Ahmed B., Solanki B., Zaidi A., Khan M.S., Musarrat J. (2019). Bacterial toxicity of biomimetic green zinc oxide nano antibiotic: insights into ZnO NP uptake and nano colloid–bacteria interface. Toxicol. Res., 8: 246.

Akhtar M.J., Ahamed M., Kumar S., Khan M.M., Ahmad J., Alrokayan S.A. (2012). Zinc oxide nanoparticles selectively induce apoptosis in human cancer cells through reactive oxygen species. Int. J. Nanomed., 7: 845–857.

Alagawany M., Qattan S.Y., Attia Y.A., El-Saadony M.T., Elnesr S.S., Mahmoud M.A., Abd El-Hack M.E., Reda F.M. (2021). Use of chemical nano-selenium as an antibacterial and antifungal agent in quail diets and its effect on growth, carcasses, antioxidant, immunity and caecal microbes. Animals, 11: 3027.

Alam M. (2021). Photocatalytic activity of biogenic zinc oxide nanoparticles: *In vitro* antimicrobial, biocompatibility, and molecular docking studies. Nanotech. Rev., 10: 1079–1091.

Alekish M., Ismail Z.B., Albiss B., Nawasrah S. (2018). *In vitro* anti-

bacterial effects of zinc oxide nanoparticles on multiple drug-resistant strains of *Staphylococcus aureus* and *Escherichia coli*: An alternative approach for antibacterial therapy of mastitis in sheep. Vet. World, 11: 1428–1432.

Al-Gabri N.A., Saghir S.A., Al-Hashedi S.A., El-Far A.H., Khafaga A.F., Swelum A.A., El-Tarabily K.A. (2021). Therapeutic potential of thymoquinone and its nanoformulations in pulmonary injury: a comprehensive review. Inter. J. Nanomed., 16: 5117.

Amaro F., Morón Á., Díaz S., Martín-González A., Gutiérrez J.C. (2021). Metallic nanoparticles—friends or foes in the battle against antibiotic-resistant bacteria?. Microorganisms, 9: 364.

Anjum S., Hashim M., Malik S.A., Khan M., Lorenzo J.M., Abbasi B.H., Hano C. (2021). Recent advances in zinc oxide nanoparticles (ZnO NPs) for cancer diagnosis, target drug delivery, and treatment. Cancers, 13: 4570.

Ashour E.A., Abd El-Hack M.E., Shafi M.E., Alghamdi W.Y., Taha A.E., Swelum A.A., El-Saadony M.T. (2020). Impacts of green coffee powder supplementation on growth performance, carcass characteristics, blood indices, meat quality and gut microbial load in broilers. Agriculture, 10: 457.

Awwad A.M., Amer M.W., Salem N.M., Abdeen A.O. (2020). Green synthesis of zinc oxide nanoparticles (ZnO-NPs) using *Ailanthus altissima* fruit extracts and antibacterial activity. Chem. Inter., 6: 151–159.

Babele P.K. (2019). Zinc oxide nanoparticles impose metabolic toxicity by de-regulating proteome and metabolome in *Saccharomyces cerevisiae*. Toxicol. Rep., 6: 64–73.

Bascheraa M., Cernelaa N., Stevensa M.J.A., Liljander A., Jores J., Cormand V.M., Nüesch-Inderbinena M., Stephana R. (2019). Shiga toxin-producing *Escherichia coli* (STEC) isolated from fecal samples of African dromedary camels. One Health, 7: 100087.

Bratz K., Golz G., Riedel C., Janczyk P., Nockler K., Alter T. (2013). Inhibitory effect of high-dosage zinc oxide dietary supplementation on *Campylobacter coli* excretion in weaned piglets. J. Appl. Microbiol., 115: 1194–1202.

Brayner R., Ferrari-lliou R., Brivois N., Djediat S., Benedetti M.F., Fievet F. (2006). Toxicological impact studies based on *Escherichia coli* bacteria in ultrafine ZnO nanoparticles colloidal medium. Nano Lett., 6: 866–870.

Cergole-Novella M.C., Pignatari A.C.C., Castanheira M., Guth B.E.C. (2011). Molecular typing of antimicrobial-resistant Shiga-toxin-producing *Escherichia coli* strains (STEC) in Brazil. Res. Microbiol., 162: 117–123.

Chen M.L., Hao Z., Tian Y., Zhang Q.Y., Gao P.J., Jin J.L. (2013). Different effects of six antibiotics and ten traditional Chinese medicines on Shiga toxin expression by *Escherichia coli* O157:H7. Evidence-Based Complemen. Alter. Med., 121407.

CLSI (2020). Performance Standards for Antimicrobial Susceptibility Testing. 30th ed. CLSI supplement M100. Wayne, PA, Clinical and Laboratory Standards Institute.

Crane J.K., Byrd I.W., Boedeker E.C. (2011). Virulence inhibition by zinc in shiga-toxigenic *Escherichia coli*. Inf. Immun., 79: 1696–1705.

Crane J.K., Broome J.E., Reddinger R.M., Werth B.B. (2014). Zinc protects against shiga-toxigenic *Escherichia coli* by acting on host tissues as well as on bacteria. BMC Microbiol., 14: 145.

Cui Y., Zhao Y., Tian Y., Zhang W., Lü X., Jiang X. (2012). The molecular mechanism of action of bactericidal gold nanoparticles on *Escherichia coli*. Biomaterials, 33: 2327–2333.

Day M., Doumith M., Jenkins C., Dallman T.J., Hopkins K.L., Elson R., Woodford N. (2016). Antimicrobial resistance in Shiga toxin-producing *Escherichia coli* serogroups O157 and O26 isolated from human cases of diarrheal disease in England, 2015. J. Antimicrob. Chemother., 72: 145–152.

Delannoy S., Mariani-Kurkdjian P., Bonacorsi S., Liguori S., Fach P. (2015). Characteristics of emerging human-pathogenic *Escherichia coli* O26:H11 strains isolated in France between 2010 and 2013 and carrying the *stx2d* gene only. J. Clin. Microbiol., 53: 486–92.

Dipineto L., Santaniello A., Fontanella M., Lagos K., Fioretti A., Menna L.F. (2006). Presence of Shiga toxin-producing *Escherichia coli O157:H7* in living layer hens. Letters Appl. Microbiol., 43: 293–295.

Dobrucka R., Dlugaszewska J., Kaczmarek M. (2018). Cytotoxic and antimicrobial effects of biosynthesized ZnO nanoparticles using of *Chelidonium majus* extract. Biomed Microdev., 20: 5.

El-Sayed W.S., Elbahloul Y., Saad M.E., Hanafy A.M., Hegazi A.H., ElShafei G.M.S., Elbadry M.J. (2019). Impact of nanoparticles on transcriptional regulation of catabolic genes of petroleum hydrocarbon-degrading bacteria in contaminated soil microcosms. Basic Microbiol., 59: 166–180.

El-Tarabily K.A., El-Saadony M.T., Alagawany M., Arif M., Batiha G.E., Khafaga A.F., Abd El-Hack M.E. (2021). Using essential oils to overcome bacterial biofilm formation and their antimicrobial resistance. Saudi J. Biol. Sci., 28: 5145–5156.

European Committee for Antimicrobial Susceptibility Testing (EUCAST) of the European Society of Clinical Microbiology and Infectious Diseases (ESCMID) (2000). Determination of minimum inhibitory concentrations (MICs) of antibacterial agents by agar dilution. Clin. Microbiol. Inf., 6: 9.

Farzana R., Iqra P., Shafaq F., Sumaira S., Zakia K. (2017). Antimicrobial behavior of zinc oxide nanoparticles and β-lactam antibiotics against pathogenic bacteria. Arch. Clin. Microbiol., 8: 57.

Ghazi F., Henni D.E., Benmechernene, Kihal M. (2009). Phenotypic and whole cell protein analysis by SDSPAGE for identification of dominants lactic acid bacteria isolated from Algerian raw milk. World J. Dairy Food Sci., 4: 78–87.

Guo B.L., Han P., Guo L.C., Cao Y.Q., Li A.D., Kong J.Z., (2015). The antibacterial activity of Ta-doped ZnO nanoparticles. Nanoscale Res. Lett., 10: 1047.

Hemeg H.A. (2018). Molecular characterization of antibiotic resistant *Escherichia coli* isolates recovered from food samples and outpatient Clinics, KSA. Saudi J. Biol. Sci., 25: 928–931.

Hozyen H.F., Ibrahim E.S., Khairy E.A., El-Dek S.I. (2019). Enhanced antibacterial activity of capped zinc oxide nanoparticles: A step towards the control of clinical bovine mastitis. Vet. World, 12: 1225–1232.

Ibrahim H.M., Amin R.A., Eleiwa N.Z., Rezk H.G. (2017). Antibacterial action of zinc oxide nanoparticles against *Staphylococcus aureus* in broiler breast fillet. Benha Vet. Med. J., 33: 117–122.

Islam F., Shohag S., Uddin M.J., Islam M.R., Nafady M.H., Akter A., Mitra S., Roy A., Emran T.B., Cavalu S. (2022). Exploring the journey of zinc oxide nanoparticles (ZnO-NPs) toward biomedical applications. Materials, 15: 2160.

Khodadadi E., Zeinalzadeh E., Taghizadeh S., Mehramouz B., Kamounah F.S., Khodadadi E., Kafil H.S. (2020). Proteomic applications in antimicrobial resistance and clinical microbiology studies. Inf. Drug Resist., 13: 1785.

Lajhar S.A., Brownlie J., Barlow R. (2017). Survival capabilities of *Escherichia coli O26* isolated from cattle and clinical sources in Australia to disinfectants, acids and Antimicrobials. BMC Microbiol., 17: 47.

Lee M.S., Koo S., Jeong D.G., Tesh V.L. (2016). Shiga toxins as multifunctional proteins: induction of host cellular stress responses, role in pathogenesis and therapeutic applications. Toxins, 8.

Li Z., Guob Z., Yin X., Ding S., Shen M., Zhang R., Wang Y., Xu R. (2020). Zinc oxide nanoparticles induce human multiple myeloma cell death via reactive oxygen species and Cyt-C/Apaf-1/Caspase-9/Caspase-3 signaling pathway *in vitro*. Biomed. Pharm. 122: 109712.

Lim J.I., Youn Y., Jang W., Hovde L., Carolyn J. (2017). A brief overview of *Escherichia coli* O157:H7 and its plasmid O157. J. Microbiol. Biotechnol., 20: 5–14.

Liu Y., He L., Mustapha A., Li H., Hu Z.Q., Lin M. (2009). Antibacterial activities of zinc oxide nanoparticles against *Escherichia coli*O157:H7. J. Appl. Microbiol., 107: 1193–1201.

Livak K.J., Schmittgen T.D. (2001). Analysis of relative gene expression data using real-time quantitative PCR and the 2(-Delta Delta C(T)) Methods, 25: 402–408.

Makhluf S., Dror R., Nitzan Y., Abramovich Y., Jelinek R., Gedanken A. (2005). Microwave-assisted synthesis of nanocrystalline MgO and its use as a bacteriocide. Adv. Funct. Mater., 15: 1708–1715.

Manzoor U., Siddique S., Ahmed R., Noreen Z., Bokhari H., Ahmad I. (2016). Antibacterial, structural and optical characterization of

mechano-chemically prepared ZnO nanoparticles. PLoS One, 11: e0154704.

Matuła K., Richter L., Janczuk-Richter M., (2019). Phenotypic plasticity of *Escherichia coli* upon exposure to physical stress induced by ZnO nanorods. Sci. Rep., 9: 8575.

Meng Q., Bai X., Zhao A., Lan R., Du H., Wang T., Xiong Y. (2014). Characterization of Shiga toxin-producing *Escherichia coli* isolated from healthy pigs in China. BMC Microbiol., 14: 1–14.

Mohammadi P., Abiri R., Rezaei M., Salmanzadeh-Ahrabi S. (2013). Isolation of Shiga toxin-producing *Escherichia coli* from raw milk in Kermanshah, Iran. Iran J. Microbiol., 5: 233–238.

Murinda S.E., Ibekwe A.M., Rodriguez N.G., Quiroz K.L., Mujica A.P., Osmon K. (2019). Shiga toxin–producing *Escherichia coli* in mastitis: An international perspective. Foodborne Pathogen. Dis.,16: 4.

Mwaheb M.A., Abd Al Halim L.R., Abdel-Baset T.A., Hemeda N.F. (2021). Comparative *In vitro* study of the antimicrobial activity of metal-ZnO nanoparticles against several bacterial and fungal pathogens. Novel Res. Microbiol. J., 5: 1338–1350.

Narayanan P.M., Wilson W.S., Abraham A.T., Sevanan M. (2012). Synthesis, characterization, and antimicrobial activity of zinc oxide nanoparticles against human pathogens. Bio Nanosci., 2: 329–335.

Naskar A., Lee S., Kim K. (2020). Easy one-pot low-temperature synthesized Ag-ZnO nanoparticles and their activity against clinical isolates of methicillin-resistant *Staphylococcus aureus*. Front. Bioeng. Biotechnol., 8: 216.

Nemček L., Šebesta M., Urík M., Bujdoš M., Dobročka E., Vávra I. (2020). Impact of bulk ZnO, ZnO nanoparticles and dissolved Zn on early growth stages of barley – a pot experiment. Plants (Basel), 15: 1365.

Obata F., Tohyama K., Bonev A.D., Kolling G.L., Keepers T.R., Gross L.K., Nelson M.T., Sato S., Obrig T.G. (2008). Shiga toxin 2 affects the central nervous system through receptor globotriaosylceramide localized to neurons. J. Inf. Dis., 198: 1398–1406.

Patel A., Dibley M., Mamtani M., Badhoniya N., Kulkarni H. (2010). Influence of zinc supplementation in acute diarrhea differs by the isolated organism. Int. J. Pediatr., 671587.

Ramadan M.A., Nassar S.H., Montaser A.S., El-Khatib E.M., Abdel-Aziz M.S. (2016). Synthesis of nano-sized zinc oxide and its application for cellulosic textiles, Egypt. J. Chem., 59: 523–535.

Reddy L.S., Nisha M.M., Joice M., Shilpa P.N. (2014). Antimicrobial activity of zinc oxide (ZnO) nanoparticle against *Klebsiella pneumoniae*. Pharm. Biol., 52: 1388–1397.

Ross A., Willson V.L. (2017). One-Way Anova. In: Basic and Advanced Statistical Tests. Sense Publishers, Rotterdam.

Rubab M., Oh D.H. (2020). Virulence characteristics and antibiotic resistance profiles of Shiga toxin-producing *Escherichia coli* isolates from diverse sources. Antibiotics, 9: 587.

Sheiha A.M., Abdelnour S.A., Abd El-Hack M.E., Khafaga A.F., Metwally K.A., Ajarem J.S., El-Saadony M.T. (2020). Effects of dietary biological or chemical-synthesized nano-selenium supplementation on growing rabbits exposed to thermal stress. Animals, 10: 430.

Shridhar P.B., Patel I.R., Gangiredla J., Noll L.W., Shi X., Bai J., Nagaraja T.G. (2019). DNA micro array-based genomic characterization of the pathotypes of *Escherichia coli* O26, O45, O103, O111, and O145 isolated from feces of feedlot cattle. J. Food Prot., 82: 395–404.

Siddiqi K.S., Rahman A., Husen A. (2018). Properties of zinc oxide nanoparticles and their activity against microbes. Nanoscale Res. Let., 13: 141.

Sikora P., Augustyniak A., Cendrowski K., Nawrotek P., Mijowska E. (2018). Antimicrobial activity of Al_2O_3, CuO, Fe_3O_4, and ZnO nanoparticles in scope of their further application in sing. Springer Nature Singapore Pte Ltd.

Singh S., Maurya P.K. (2019). Nanotechnology in modern animal biotechnology: Recent trends and future perspectives. Springer Nature Singapore Pte Ltd.

Stoimenov P.K., Klinger R.L., Marchin G.L., Klabunde K.J. (2002). Metal oxide nanoparticles as bactericidal agents. Langmuir, 18: 6679–6686.

Stromberg Z.R., Lewis G.L., Marx D.B., Moxley R.A. (2015). Comparison of enrichment broths for supporting growth of Shiga toxin producing *Escherichia coli*. Curr. Microbiol., 71: 214e9.

Sungkaworn T., Triampo W. Nalakarn P., Triampo D., Tang I.M., Lenbury Y. (2007). The effects of TiO_2 nanoparticles on tumor cell colonies: fractal dimension and morphological properties. Inter. J. Biomed. Sci., IJBS, 2: 67–74.

Tayel A., El-tras F., Moussa S., El-baz A., Mahrous H., Salem F., Brimer L. (2011). Antibacterial action of zinc oxide nanoparticles against foodborne pathogens. J. Food Safety, 31: 211–218.

Thangam A., Pritam M., Akshmi S.A. (2014). Effect of ZnO nano particles against strains of *Escherichia coli*. Asian J. Pharm. Clin. Res., 7: 202–206.

Torabi L.R. (2017). The antibacterial effects of ZnO nanoparticles on patients with urinary tract infection isolated from Alzahra Hospital in Isfahan, Iran. Zahedan J. Res. Med. Sci., 19: e10359.

Tsakou F., Jersie-Christensen R., Jenssen H., Mojsoska B. (2020). The role of proteomics in bacterial response to antibiotics. Pharmaceuticals, 13: 214.

Uemura R., Katsuge T., Sasaki Y., Goto S., Sueyoshi M. (2017). Effects of zinc supplementation on Shiga toxin 2e-producing *Escherichia coli in vitro*. J. Vet. Med. Sci.,79: 1637–1643.

Wagner G., Korenkov V., Judy J.D., Bertsch P.M. (2016). Nanoparticles composed of Zn and ZnO inhibit *Peronospora tabacina* spore germination *in vitro* and *P. tabacina* infectivity on tobacco leaves. Nanomaterials (Basel), 6: 50.

Wang C., Liu L., Zhang A., Xie P., Lu J., Zou X. (2012). Antibacterial effects of zinc oxide nanoparticles on *Escherichia coli* K88. African J. Biotechnol., 11: 10248–10254.

Woodhouse E.J. (2004). Nanotechnology controversies. Technol. Soc. Mag. IEEE, 23: 6–8.

Xiaolia L., Dudley E.G. (2017). A quantitative enzyme-linked immunosorbent assay for Shiga toxin 2a requiring only commercially available reagents. Adv. Food Technol. Nutr. Sci. Open J., 3: 6–14.

Yehia N., AbdelSabour M.A., Erfan A.M., Ali Z.M., Soliman R.A., Samy A., Abd El-Hack M. E., Ahmed K.A. (2022). Selenium nanoparticles enhance the efficacy of homologous vaccine against the highly pathogenic avian influenza H5N1 virus in chickens. Saudi J. Biol. Sci., 29: 2095–2111.

Yusof H.M., Mohamad R., Zaidan U.H., Rahman N.A. (2019). Microbial synthesis of zinc oxide nanoparticles and their potential application as an antimicrobial agent and a feed supplement in animal industry: a review. J. Anim. Sci. Biotechnol., 10: 1–22.

Zhang L., Jiang Y., Ding Y., Daskalakis N., Jeuken L., Povey M., O'Neill A.J., York D.W. (2010). Mechanistic investigation into antibacterial behaviour of suspensions of ZnO nanoparticles against *E. coli*. J. Nanopart. Res., 12: 1625–1636.

Received: 24 X 2022
Accepted: 15 XI 2022